# Lawrence Berkeley National Laboratory

## Lawrence Berkeley National Laboratory

**Title**

Microhole arrays for improved heat mining from enhanced geothermal systems

**Permalink**

https://escholarship.org/uc/item/171592zr

**Author**

Finsterle, S.

**Publication Date**

2013-02-01

eScholarship.org Powered by the California Digital Library
University of California

# Microhole arrays for improved heat mining from enhanced geothermal systems

Stefan Finsterle [a], Yingqi Zhang [a,*], Lehua Pan [a], Patrick Dobson [a], Ken Oglesby [b]

[a] Earth Sciences Division, Lawrence Berkeley National Laboratory, 1 Cyclotron Road, MS 74-120, Berkeley, CA 94720, USA
[b] Impact Technologies LLC, Tulsa, OK 74153, USA

Keywords:
Geothermal energy
Heat extraction
Microholes
Numerical modeling
EGS

abstract

Numerical simulations are used to examine whether microhole arrays have the potential to increase the heat mining efficiency and sustainability of enhanced geothermal systems (EGS). Injecting the working fluid from a large number of spatially distributed microholes rather than a few conventionally drilled wells is likely to provide access to a larger reservoir volume with enhanced overall flow distances between the injection and production wells and increased contact area between permeable fractures and the hot rock matrix. More importantly, it reduces the risk of preferential flow and early thermal breakthrough, making microhole array-based EGS a more robust design. Heat recovery factors are calculated for EGS reservoirs with a conventional well configuration and with microhole arrays. The synthetic reservoir has properties similar to those of the EGS test site at Soultz-sous-Forêts. The wells and microholes are explicitly included in the numerical model. They intersect a stimulated reservoir region, which is modeled using a dual-permeability approach, as well as a wide-aperture zone, which is incorporated as a discrete feature. Local and global sensitivity analyses are used to examine the robustness of the design for a variety of reservoir and operating conditions. The simulations indicate that the flexibility offered by microhole drilling technology could provide an alternative EGS exploitation option with improved performance.

## 1. Introduction

Geothermal energy is considered to be a clean, carbon-neutral, renewable and stable form of baseload energy. High-enthalpy heat mining for electrical energy production requires systems consisting of (1) a heat source with sufficiently high temperature at accessible depths, (2) fluids to absorb the heat from the hot rock matrix and to transport it to the surface, and (3) interconnected pore space that allows fluid flow at acceptably high rates between injection and production wells. While heat is present essentially everywhere in the subsurface (MIT, 2006), the requirements for sufficient water and permeability are only met at locations where the tectonic, structural, and geologic conditions favor the development of a hydrothermal system. In the absence of such favorable conditions, the concept of enhanced geothermal systems (EGS) provides a means to create a reservoir by hydraulically or thermally fracturing the rock or shearing existing fractures, thus generating or increasing permeability and inter-well connectivity. The injected working fluids then pick up reservoir heat as they flow along the created permeable pathways toward production wells.

The fact that an EGS reservoir needs to be engineered by drilling wells for stimulation, injection, and production leads to considerable technical challenges, but at the same time provides unique opportunities to design and optimize the system for maximum heat extraction and sustainability at minimum risk and cost. Advances in drilling technology are essential for the technical success and economic viability of EGS. Specifically, the development of drilling technology for slimholes (bores less than 6½ inches or 16.5 cm diameter), microholes (bores less than 4 inches or 10.2 cm diameter), or ultra-slim diameter wells (bores between 1 and 3 inches (2.5 and 7.4 cm) diameter) (Pritchett, 1998; Finger et al., 1999; Moe and Rabben, 2001; Garg and Combs, 2002; Sanyal et al., 2005) may offer the flexibility needed to design well configurations that enable optimization of geothermal heat mining using EGS.

Pritchett (1998) showed considerable potential of slimhole drilling for smaller geothermal projects (100–1000 kWe) in off-grid remote areas. Slimhole drilling technology for the operation of small geothermal power plants is summarized in the Slimhole Handbook (Finger et al., 1999), which contains case studies and recommendations for slimhole drilling practice. Moreover, the U.S. Department of Energy sponsored a Microhole Initiative to promote the development of technology and tools for microhole drilling where the advanced FLASH ASJ™ drilling technology for microhole drilling was developed (Oglesby, 2009; Summers et al., 2007).

* Corresponding author. Tel.: +1 510 495 2983; fax: +1 510 486 5686.
E-mail address: YQZhang@lbl.gov (Y. Zhang).

Only a few drilling techniques can complete microholes because the small bore reduces the size of the drillpipe that can be used. A small drillpipe has less torque capabilities, less weight on bit and reduced flow rates for drilling. Cleaning of drill cuttings and well control can also pose difficult issues. However, the benefits of smaller bores are that they allow for smaller rigs, pipes, and tools, thus requiring less energy (and cost).

Maurer (1980) and others have reported on advanced techniques that have the potential to drill microholes. While high-pressure water jetting has limited capabilities in drilling into medium-to-hard rocks, supercritical fluid abrasive slurry jet drilling technology (FLASH ASJ™, Impact Technology, Tulsa, Oklahoma) has been shown to drill through hard rocks, including basalt, in bench tests; the technology is now being tested in shallow field conditions. Because it is an abrasive cutting technology, it allows a very simple downhole assembly, requires no rotation or weight on bit to drill through rocks and steel at high rates of penetration (ROP). It can utilize continuous coiled tubing for faster tripping into and out of the bore and better well control because it has no threaded joints. This is an underbalanced or managed pressure drilling technology that is likely to be cost-effective due to its reduced mud and chemical usage and disposal, smaller tubulars and small rigs, with shorter drilling times as a result of higher ROP and the absence of down times for joint connections.

Currently there are some limitations with inserting microholes under EGS conditions. While the depth, azimuth and inclination at the kick off point in the main large-diameter borehole can be well controlled (Johnson and Hyatt, 2005), microhole drilling has limited capabilities for real-time adjustment of azimuth and inclination due to the small pipe diameters, which cannot accommodate large directional measurement tools. Nevertheless, the controllable microhole orientation at the kick-off point and the known effects of gravity, pipe strength (or allowable bend angle) and ROP allow for some directional drilling capabilities, sufficient to generate an array of a specific layout. This technique was successfully utilized in the early development of oilfield directional drilling (see Heuze (1995) and references therein).

While microholes have mainly been used for exploration, sampling, monitoring and resource assessment purposes (Garg and Combs, 1997; Albright and Dreesen, 2000), other uses within EGS projects can be envisioned. For example, the hydraulic, thermal or chemical stimulation of a reservoir from many points within a microhole array could create fracture networks that are more extensive and with enhanced connectivity. Even if it is infeasible or ineffective to use microhole arrays for reservoir stimulation, multiple microholes used as injection or production wells could more flexibly target the zone in the reservoir that is (conventionally) stimulated by hydroshearing of critically stressed fractures (as revealed by microseismicity). Moreover, the probability of intersecting the portion of the fracture network that is actually connected to the wells is greatly increased when using multiple, potentially inclined and directionally drilled microholes compared to the probability obtained when using a small number of larger diameter conventional wells. High accuracy in directional microhole drilling, however, is not considered an essential requirement, as it is an inherent aspect of the proposed concept that the locations of feedzones are essentially unknown and cannot be targeted by designed well trajectories. Instead, these zones are included in the heat-mining process through the generation of a hydraulic potential field of large extent, wherein the working fluid finds the connectivity between the injection and production wells.

Sanyal et al. (2005) proposed to inject water through multiple ultra-slim holes at relatively low flow rates with the goal of preheating the working fluid. In such a system, rather than relying entirely on heat transfer occurring in the stimulated fracture network, the well array itself is used as the main heat exchanger, i.e., heat is transferred mainly by conduction from the hot rock matrix to the fluid contained in the wells, with the exception of a short flow distance from the tips of the ultra-slim holes through a thermally stimulated fracture network to a central production well.

We use the term "microhole" to refer to any borehole that is of considerably smaller diameter than a conventional geothermal injection or production well, and that can be drilled relatively cheaply so that an array of multiple such holes can be completed in a cost-effective manner.

The objective of this study is to examine the potential of microholes – used as injection or production wells – to improve the efficiency and sustainability of geothermal energy production as compared to EGS with a conventional well configuration. We test the hypotheses that this improved performance is achieved because (1) microholes that emanate from a central larger well (potentially at different elevations) can be spread widely (both horizontally and vertically), so they intersect a larger portion of the hot reservoir and its fracture network, thus increasing the rock volume that is accessed by the circulating working fluid; (2) the spatial distribution of injection or production rates can be manipulated by flexible well placement, i.e., flow patterns in the reservoir can be partly controlled to maximize the volume encountered by the working fluid, and to minimize the risk of early thermal breakthrough; (3) injection and/or production rates are partly self-regulated by the velocity-dependent flow resistance in the microholes, reducing the risk of early thermal breakthrough; and (4) flow velocities through the microholes and the fractured formation are generally reduced (as the combined flow area of multiple microholes is greater than that of conventional large-diameter wells) leading to increased uptake of heat from the rock matrix.

These hypotheses are examined through numerical modeling of a synthetic EGS reservoir, which is modeled after (but does not represent) the conditions at the European EGS test site at Soultz-sous-Forêts, France (e.g., Gérard and Kappelmeyer, 1987; Sausse et al., 2010). Temperatures and recovery factors are calculated for a conventional well configuration and one based on microhole arrays, and sensitivity analyses are performed to examine the key factors and robustness of the proposed concept.

These analyses are based on the fundamental assumption that microhole drilling technology will advance to a stage where it can be cost-effectively deployed under geothermal reservoir conditions. A detailed discussion of the requirements, challenges, and current state of the development of such a drilling technology and its costs to employ is outside the scope of this article. This precludes us from performing an economic analysis; instead, we approach the question whether microhole-based EGS is viable from the perspective of the physical system, which (if successful) then provides the constraints for the economic feasibility analysis. Furthermore, we do not discuss the potential use of microholes for reservoir stimulation. The key objective of this article is to examine the potential benefits that could be derived by the development of a cost-effective microhole technology for EGS applications.

## 2. Model development and analysis methods

### 2.1. Reservoir model

The comparison of EGS performance using conventional and microhole well configurations is based on numerical simulations. The reservoir model developed for this purpose has characteristics similar to those encountered at the European EGS demonstration site in Soultz-sous-Forêts, France. However, this is strictly a synthetic modeling study, and no conclusions about the potential performance of microholes at the test site should be drawn from this analysis, as the model is a highly simplified representation

**Table 1**
Base-case model parameters and ranges examined in global sensitivity analysis.

| Parameter | Value | Range | |
|---|---|---|---|
| $Log_{10}$ (permeability wide-aperture zone [$m^2$]) | −10.0 | −11.0 | −9.0 |
| $Log_{10}$ (permeability fractures horizontal [$m^2$]) | −13.0 | −14.0 | −12.0 |
| $Log_{10}$ (permeability fractures vertical [$m^2$]) | −13.0 | −14.0 | −12.0 |
| $Log_{10}$ (permeability matrix [$m^2$]) | −18.0 | −20.0 | −16.0 |
| Volume fraction[a] wide-aperture zone fracture continuum | 0.02 | 0.01 | 0.05 |
| Volume fraction[a] reservoir fracture continuum | 0.005 | 0.001 | 0.01 |
| Porosity[b] wide-aperture fracture continuum | 0.5 | n/a[c] | n/a[c] |
| Porosity[b] reservoir fracture continuum | 0.5 | n/a[c] | n/a[c] |
| Porosity[b] matrix continuum | 0.05 | 0.02 | 0.1 |
| Fracture spacing [m] | 30.0 | 10.0 | 100.0 |
| $Log_{10}$ (fracture-matrix area reduction factor) | −1.0 | −2.0 | 0.0 |
| Rock grain density [$kg\,m^{-3}$] | 2600. | n/a[c] | n/a[c] |
| Thermal conductivity [$W\,m^{-1}\,°C^{-1}$] | 3.0 | 2.5 | 3.5 |
| Heat capacity [$J\,kg^{-1}\,°C^{-1}$] | 950.0 | 900.0 | 1000.0 |
| Injection rate [$kg\,s^{-1}$] | 80.0 | 40.0 | 120.0 |
| Injection temperature [°C] | 50.0 | 25.0 | 75.0 |

[a] The volume fraction of the matrix continuum, $f_{V,m}$, is linked to that of the fracture continuum, $f_{V,f}$, by $f_{V,m} = (1-f_{V,f})$.
[b] Continuum porosity is defined as the fracture or matrix pore volume divided by volume of the respective continuum. In the dual-permeability approach, the total fracture or matrix porosity, defined as the fracture or matrix pore volume divided by the bulk volume, is the product of the volume fraction and the respective continuum porosity.
[c] n/a = not applicable; corresponding parameter is fixed, i.e., not included in sensitivity analyses.

of the conditions at Soultz-sous-Forêts. Moreover, a range of formation properties will be considered to examine the robustness of the microhole design to variability and uncertainty in reservoir conditions.

The model domain consists of a rectangular cuboid of dimensions 2.0 km × 3.0 km × 1.5 km, positioned at a depth between 3.8 and 5.3 km. The temperatures at the impermeable top and bottom boundaries of the model domain are fixed at 160 °C and 200 °C, respectively; this provides heat input into the system after energy extraction begins. Initial pressures vary hydrostatically from about 3.7 MPa at the top to about 5.1 MPa at the base. Within this block of low-permeability rock lies the EGS reservoir, consisting of a zone of fractures that were created or reactivated by hydraulic stimulation. The shape and size of this zone is approximately taken from the cloud of micro-seismic events recorded at Soultz-sous-Forêts (Michelet and Toksöz, 2007; Cuenot et al., 2008); the zone is assumed to be a horizontal, approximately elliptical region with a length and width of about 2.0 km and 1.0 km, respectively, and a thickness of 0.4 km, located at a depth between 4.4 and 4.8 km. The EGS reservoir is represented by a dual-permeability model, where permeable fractures and the essentially impermeable rock matrix are modeled as overlapping interacting continua. This is an extension of the classical double-porosity model (Warren and Root, 1963), with global heat flow through the matrix continuum added to global fracture flow and the interaction between the fracture and matrix continua. It is a specific case of the multiple interacting continua approach (MINC; Pruess and Narasimhan, 1982, 1985) in that the matrix continuum is not subdivided into multiple elements. A detailed discussion of various ways to numerically represent fracture-matrix systems can be found in Doughty (1999).

Finally, within the fractured EGS reservoir, we add a highly permeable, planar wide-aperture feature as a potential zone for preferential flow between the injection and production wells. We define the slightly inclined plane by the points of highest injectivity observed during hydraulic testing at Soultz-sous-Forêts (Sausse et al., 2010); it is assumed to extend across the entire stimulated reservoir.

The key heat mining process can be described as conductive heat transfer between the hot rock matrix and the working fluid flowing through the fracture network; this sustains the convective transport of heated fluid to the production well. The overall effectiveness of the conductive heat transfer depends on the contact area between the rock and the working fluid, which as a first approximation can be taken as the total fracture surface area. However, due to heterogeneity in the aperture distribution of individual fractures and that of the fracture network itself, it is unlikely that the working fluid migrates uniformly from the injection well to the production well; it is thus improbable that it encounters the entire geometric fracture surface area along its flow path. Interpretations of tracer test data and related modeling at Soultz (Vogt et al., 2012) suggest that flow is channelized, and considerable portions of the fracture network are being bypassed, reducing contact area and heat transfer from the reservoir rock to the working fluid. Preferential flow paths may also develop as a result of coupled thermo-mechanical effects that induce differential reservoir cooling (McDermott et al., 2006). Grant and Garg (2012) compared the heat recovery factors calculated by the double-porosity model of Sanyal and Butler (2005) with estimates from hydrothermal systems (Garg and Combs, 2010) and concluded that the model-calculated values are too optimistic as they do not account for flow channeling effects. These studies suggest that the actual contact area available for heat transfer is substantially smaller than the geometric fracture surface area, which is calculated from fracture spacing information for the dual-permeability model. We therefore include a contact area reduction factor and apply it to the dual-permeability regions (i.e., stimulated EGS reservoir and high-permeability zone) of our model. This approach is similar to the Active Fracture Model concept introduced by Liu et al. (1998) for unsaturated and two-phase flow in fractured porous media.

Table 1 summarizes some key model parameters. Ranges are provided for those parameters that will be evaluated in a global sensitivity analysis to examine their impact on the calculated heat mining efficiency.

EGS performance is simulated using the non-isothermal, multiphase, multicomponent flow and transport code TOUGH2 (Pruess et al., 1999; http://esd.lbl.gov/TOUGH), which solves the governing mass and energy conservation equations using the integral finite difference method (Narasimhan and Witherspoon, 1976) in a fully coupled manner. Appendix A summarizes the mathematical model solved by the TOUGH2 simulator.

In summary, the reservoir model described in this section is considered of sufficient complexity for its intended purpose of evaluating the relative heat-mining efficiencies of the conventional and microhole well designs. It appropriately simulates the relevant flow processes in fracture-porous media and in wells, and includes an accurate description of the thermophysical properties. Key features of an EGS reservoir are represented, specifically the presence of low-permeability cap- and base-rock zones that

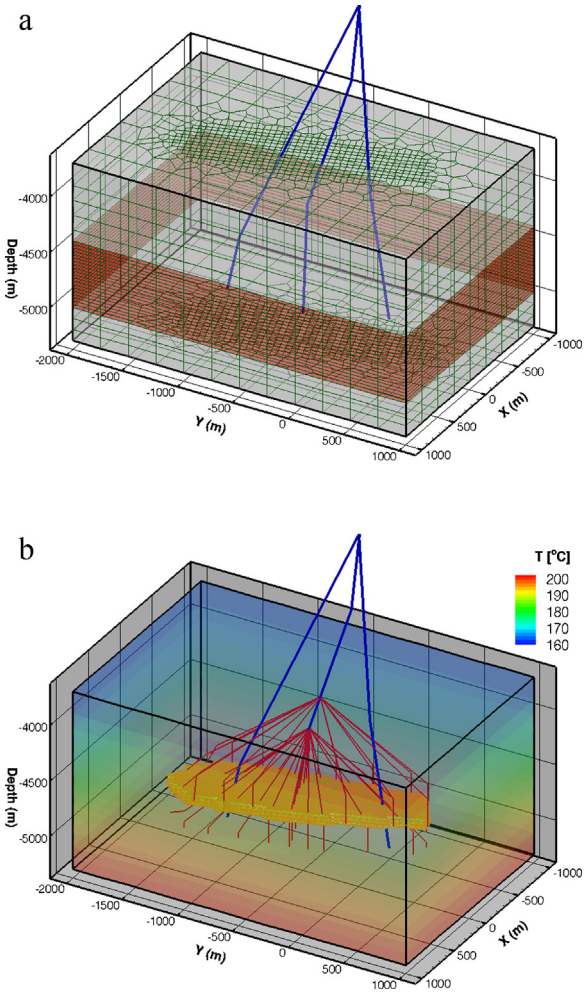


**Fig. 1.** Simulated borehole configurations: (a) conventional wells, numerical grid on model domain faces, with unstructured portion indicating projection of elliptical EGS reservoir (model layer containing reservoir is highlighted); (b) microhole arrays, initial temperature distribution, and wide-aperture zone.

bound the reservoir, the stimulated, fractured reservoir embedded in a unfractured, native formation, and a wide-aperture zone potentially acting as a fast-flow path. Fluid and heat transfer between fractures and the rock matrix are accounted for using the dual-permeability approach. Moreover, flow-channeling effects are included, which are the result of sub-grid-block heterogeneity within the fracture network. Finally, conventional wells and microholes are explicitly discretized in the model to capture near-well effects. While large-scale and sub-grid-block scale heterogeneities are accounted for, it is obvious that additional features and intermediate-scale heterogeneities are present in a real reservoir. They are likely to affect the actual production behavior and are thus frequently incorporated into reservoir models as part of the calibration process. Looking at the impact of such features on the relative heat-mining efficiencies is beyond the scope of this conceptual study, but is expected to be a second-order effect that may further demonstrate the appeal of a microhole-based EGS design.

### 2.2. Well configurations

We compare EGS heat mining performance using two distinct well configurations (Fig. 1). The first configuration consists of conventionally drilled, large-diameter injection and production wells in an arrangement similar to that used at Soultz-sous-Forêts (Fig. 1a). This model consists of three conventional wells directionally drilled from a single well pad. The wells reach the target formation at a depth between 4.5 and 5.0 km, with a bottom hole separation distance of about 600 m. Cold water is injected into the central well with a downhole completion diameter of 0.216 m; hot water is produced from the two peripheral wells, which have respective diameters of 0.178 m and 0.216 m.

In the second configuration (Fig. 1b and Fig. 2), 40 microholes of diameter 0.064 m emanate in two arrays from a conventionally drilled well. Thirty-four of the 40 microholes are drilled such that their end points circumscribe the outer edge of the stimulated zone, with the remaining six microholes terminating on the short axis of the elliptical fracture zone (i.e., the pattern of the end points of the microhole arrays resembles the Greek character θ). The kickoff angle of the microholes is 45° from the axis of the central well. While most likely curved in a real application, we assume that they are drilled straight until they reach their final position in the X-Y plane, at which point they become vertical. Each microhole is approximately 1 km long. The first array of 13 microholes kicks off at a depth of 3.8 km; this array comprises the microholes that need to reach the outermost portion of the EGS reservoir. The second array consists of the remaining 27 microholes, which emanate from the conventional well at a depth of 4.1 km.

The microholes are used for injection; two conventional wells are used for production. The conventional wells are the same as those shown in Fig. 1a, except that the central well is shorter, terminating at the lowest microhole kickoff point at a depth of 4.1 km. This microhole pattern is obviously only one design out of a large number of potential alternative configurations. Optimization of the microhole array geometry is not part of the current study, but is certainly recommended once the viability of the basic approach has been demonstrated.

The conventional wells and the microholes are explicitly discretized in our numerical model, albeit in a simplified manner. Following the trajectory of the borehole, cylindrical grid blocks are inserted into the existing elements of the basic grid (Fig. 1a shows the basic grid on the faces of the model domain, where the unstructured, elliptical part indicates the location of the EGS reservoir). These well elements are connected to each other in the axial direction and to the elements in which they are embedded. The conventional wells are perforated only within the stimulated reservoir zone; the microholes are uncased and thus connected to the formation over their entire length. In the base case, wellbore flow is calculated using the standard Darcy law with an effective permeability, which is determined for the expected flow velocities using a wellbore simulator that is integrated into the TOUGH2 code, calculating the transient non-isothermal wellbore flow using the drift-flux model (Pan et al., 2011). For the wellbore sections above the model domain, i.e., from the land surface to a depth of 3.8 km, a semi-analytical solution for radial heat exchange with the surrounding formation is used (Zhang et al., 2011) to efficiently calculate heating of the injected water and heat losses from the produced water as it flows along the wells through rocks that exhibit a geothermal gradient. Given the relatively long vertical flow distance in these wellbore sections, the gravitational potential is added to the energy balance equation (Stauffer et al., 2003). This effect, which is similar in magnitude to the temperature changes caused by the negative Joule-Thomson coefficient of water, is added to avoid an overprediction of the temperature and heat content of the produced fluid.

### 2.3. Performance measures

The comparison of conventional and microhole-based EGS is made using a simple performance measure, which is the heat recovery factor at the end of a 30-year exploitation period. The heat

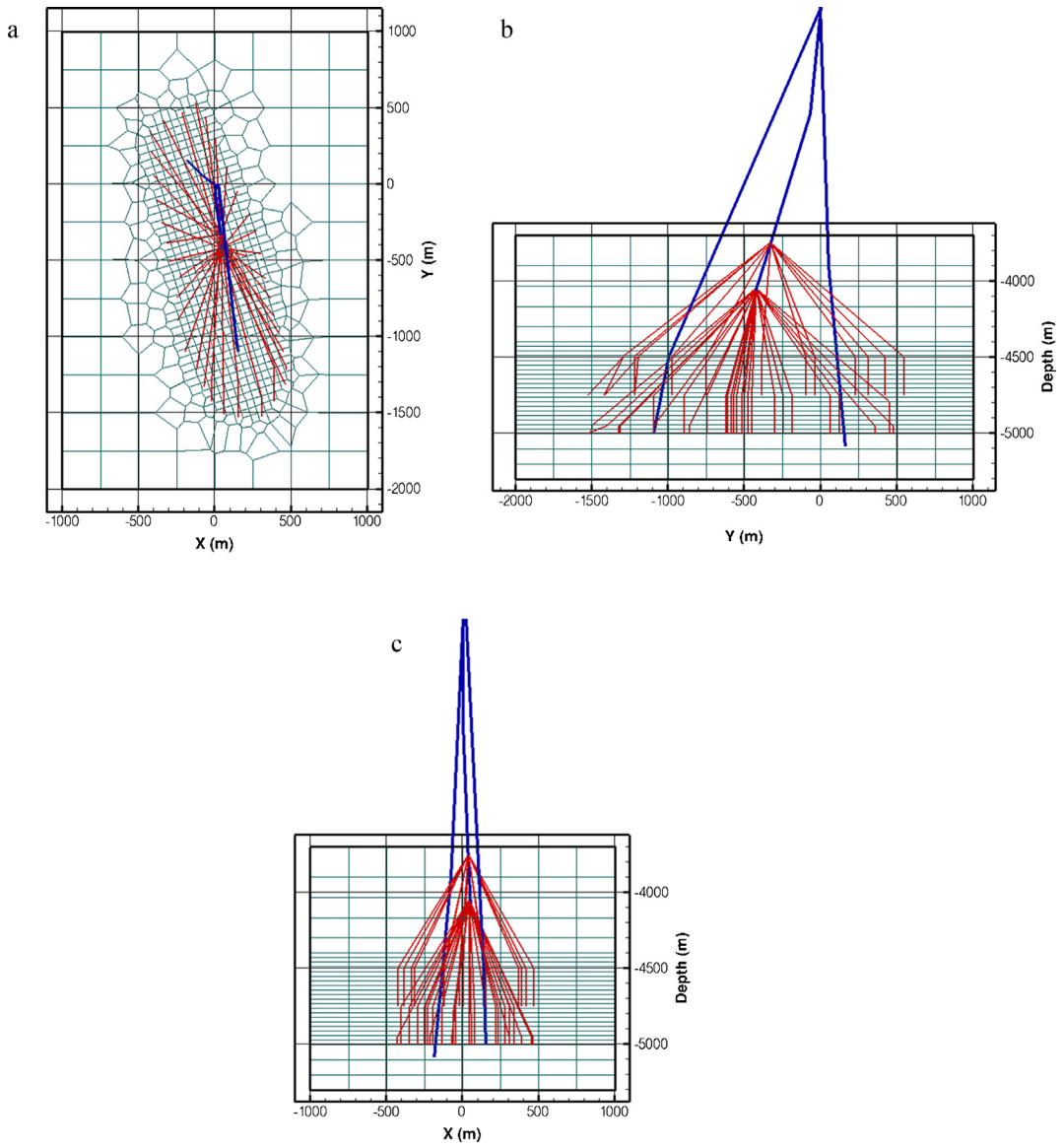


**Fig. 2.** Plan and cross-sectional views of microhole configuration with conventional wells shown in blue and microholes shown in red. The numerical mesh is shown in green. For the well sections above the numerical mesh, a semi-analytical radial heat-exchange model is used. (For interpretation of the references to colour in this figure legend, the reader is referred to the web version of this article.)

recovery factor is defined as the cumulative heat recovered at the well head divided by the initial heat in the reservoir, $E_0$:

$$F = \frac{\int (q_p h_p - q_i h_i) dt}{E_0} = \frac{\Delta E}{E_0} \quad (1)$$

Here, $q_p$ and $q_i$ are the mass production and injection rates, and $h_p$ and $h_i$ are the enthalpies of the produced and injected fluids, respectively. The net energy extracted from the reservoir, $\Delta E$, can be used to assess the electrical production potential of the well system, and since the initial energy stored in the reservoir is a constant and the same in both considered scenarios, the heat recovery factor is also a measure of long-term sustainability of the system. In addition to the heat recovery factor as an integral performance measure, we also monitor the thermal drawdown in the production wells as a function of time.

Evaluating these measures for the base-case parameter set shown in Table 1 provides some initial indication of the relative performance of systems that use conventional wells or microholes. However, such an analysis is necessarily based on a number of assumptions about the properties of the stimulated reservoir. These assumptions are associated with considerable uncertainty. We therefore also report a criterion that examines the robustness of the system to uncertainty in model parameters. We consider it advantageous if energy production is relatively insensitive to the details of reservoir properties such as fracture spacing, permeability of the wide-aperture zone, and other thermo-hydrological properties. Given the computational demands of a single simulation run and the high dimension of the parameter space, it is impossible to exhaustively sample all likely parameter combinations. As an alternative, we perform a global sensitivity analysis and examine the elementary effect (defined as the change of model output due to a perturbation in one of the model inputs) and its standard deviation as qualitative measures of relative sensitivities and overall robustness of the respective well configurations. The sensitivity analysis methods used are briefly described in the following subsection.

### 2.4. Sensitivity analysis methods

We use two sensitivity analysis approaches in this study. The first approach is a simple local method, which evaluates sensitivity coefficients at a single point in the parameter space (the base-case parameter set of Table 1), and which provides some statistical correlation coefficients among the parameters. The second approach is a global method, which examines elementary effects within a parameter hypercube, and which can also indicate the degree of nonlinearity and interdependence of model parameters.

In the local sensitivity analysis, we simply evaluate the matrix of partial derivatives of the performance measures, $z$, with respect to the parameters of interest, $p$. To make the elements of this matrix dimensionless and thus comparable with each other, they are scaled by a potential parameter variation, $\sigma_p$, and by a standard deviation of the performance measure, $\sigma_z$, which can be interpreted as the change in the outcome that would be considered significant:

$$S_{ij} = \frac{\partial z_i}{\partial p_j} \cdot \frac{\sigma_{pj}}{\sigma_{z_i}} = J_{ij} \cdot \Gamma_{ij} \tag{2}$$

Taking the sum of the absolute values of a column or row of the scaled sensitivity matrix **S** provides some overall indication of the relative sensitivity of the corresponding performance measure or the relative influence of the corresponding parameter, respectively.

The covariance matrix of the parameters is given by

$$\mathbf{C}_{pp} = (\mathbf{J}^T \mathbf{C}_{zz}^{-1} \mathbf{J})^{-1} \tag{3}$$

where $\mathbf{C}_{zz}$ holds the variances $\sigma_z^2$ on its diagonal. In this study, we use Eq. (3) mainly to calculate the correlation coefficients among pairs of parameters, i.e.,

$$r_{ij} = \frac{c_{ij}}{\sqrt{c_{ij} \cdot c_{jj}}} \quad -1 \le r_{ij} \le 1 \tag{4}$$

where the variances and covariances $c_{ij}$ are the elements of matrix $\mathbf{C}_{pp}$.

As stated above, this sensitivity analysis is local in the sense that it is valid for a specific point in the parameter space. If the model is nonlinear, however, sensitivity coefficients are different for each parameter combination. Global sensitivity analysis methods address this issue by examining many combinations within the range of acceptable parameter values. Saltelli et al. (2008) describe available global sensitivity analysis approaches. The variance-based methods require a very large number of model evaluations and are thus not practical for computationally expensive models as those used to simulate EGS performance of fractured reservoirs using microhole arrays. However, the method originally proposed by Morris (1991) serves the purpose of providing qualitative measures of relative parameter influence and nonlinearity with a manageable number of simulation runs. In this approach (which is commonly referred to as the Morris one-at-a-time (MOAT) elementary effects method), each axis of the parameter hypercube is subdivided into $k-1$ intervals for a total of $k^n$ grid points, where $n$ is the number of parameters. A perturbation $\Delta$ is then calculated for each parameter $i$:

$$\Delta_i = \frac{k}{2(k-1)} \cdot (p_{i,\max} - p_{i,\min}) \tag{5}$$

Next, a random grid point in the parameter space is selected, the model is run and the performance measure $z$ is evaluated. Then – one at a time and in random order – each parameter $p_i$ is perturbed by $\Delta_i$, the model is run to recalculate $z$, and the corresponding impact (or elementary effect, $EE_i$) on the output is computed as

$$EE_i = \frac{z(p_1, p_2, \ldots, p_{i-1}, p_i + \Delta, \ldots, p_n) - z(p_1, p_2, \ldots, p_n)}{\Delta} \tag{6}$$

The procedure is repeated for multiple, randomly selected starting points of a path in the parameter space that consists of $n$ steps and $n+1$ simulation runs for the evaluation of the elementary effect in the vicinity of this point. After completion of a number of such paths, which is mainly determined by computational limitations, the mean and standard deviation of the absolute elementary effects are calculated. The mean assesses the overall influence of the respective parameter on the output; the standard deviation indicates whether the effects are linear and additive or nonlinear, or whether interactions among the parameters are involved.

The iTOUGH2 code (Finsterle, 2004; http://esd.lbl.gov/iTOUGH2), which is the inverse modeling and uncertainty analysis tool for TOUGH2, is used to perform TOUGH2 simulations of EGS performance and to perform local and global sensitivity analyses. If parameters of a pre-processor are varied as part of the analysis (as is done here for the parameters of the dual-permeability model, which enter the mesh generator), the PEST protocol is employed, as described in Finsterle and Zhang (2011). All simulations for the local and global sensitivity analysis are independent from each other and thus can be run in parallel, supported by iTOUGH2-PVM (Finsterle, 1998).

## 3. Results and discussion

### 3.1. Fluid and heat flow in microholes

Before we present the results that represent the total system performance (i.e., the overall heat-mining efficiency), we discuss some details of fluid flow and heat transfer in the microholes. First, we examine the preheating effect, which was previously described by Sanyal et al. (2005). To demonstrate the preheating effect for the well configuration of our study, we developed a submodel that considers fluid flow through a 4 km long conventional well of radius 0.1 m, which is connected to forty 1.3 km long microholes of radius 0.032 m. The microholes fan out symmetrically from the central well at a 45° angle for 1 km, and then become vertical for the remaining 300 m. This submodel is very similar to the actual configuration studied in the 3D model. Water of 50 °C is injected at a rate of 80 kg/s; each microhole takes 2 kg/s, assuming symmetry. Fluid exits the well system at the bottom of the microholes, which is different from the scenario studied in the full model, where water may exit the microhole at any location according to the local injectivity. The formation temperature follows a geothermal gradient of 30 °C/km. Assuming that preheating of the working fluid in the injection well system occurs by radial heat conduction only, and that there is no interference among the microholes, we can employ a semi-analytical solution for calculating transient, radial heat exchange between a flowing wellbore and a conductive formation (Zhang et al., 2011). The results are presented in Fig. 3. It demonstrates that preheating of the large-diameter conventional well is relatively small (approximately 6 °C over a flow distance of 4 km). Once the fluid enters one of the microholes, the temperature increases from 55 to above 100 °C at early times, i.e., significantly more than in the upper part of the well system despite the shorter flow distance. This is due to several factors, notably the smaller flow velocity in the microholes (0.55 m/s) compared to that in the large-diameter section of the injection system (2.2 m/s), which substantially increases the heat uptake. Moreover, the microholes are located in the deeper parts of the reservoir and thus encounter higher rock temperatures. The inclination of the microholes also contributes to the preheating effect, as it prolongs the length of the flow path to reach the target depth. However, as time goes on, cooling of the rock around the microholes gradually reduces the preheating effect, with temperatures dipping below 100 °C after about 4 years. After 30 years, the temperature reaches about 90 °C,

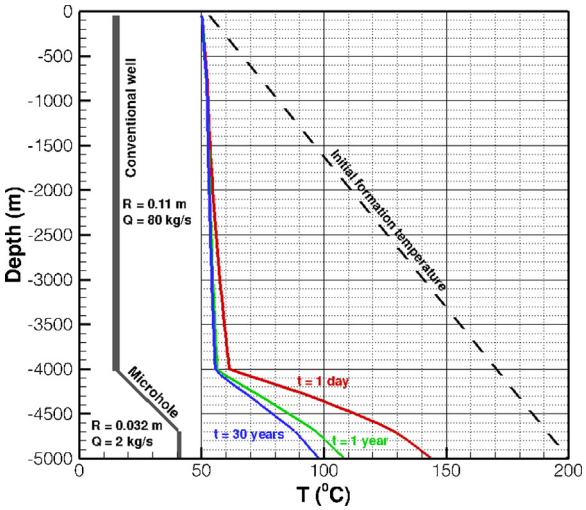


**Fig. 3.** Conductive preheating of working fluid in an injection system consisting of a large-diameter well connected to 40 inclined microholes (only one microhole is shown due to symmetry).

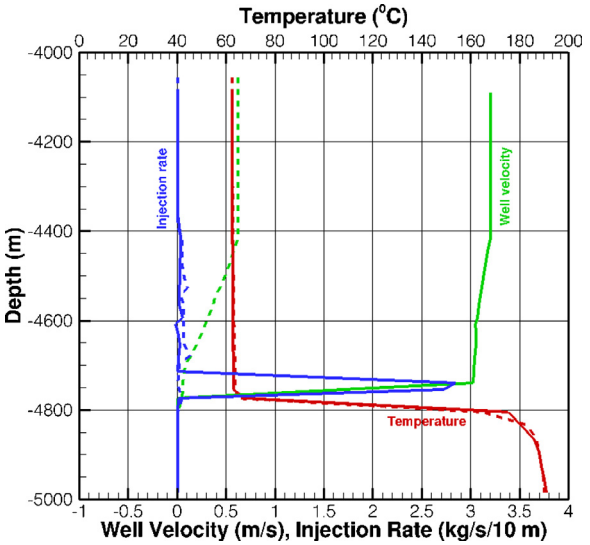


**Fig. 4.** Distribution of temperature (red lines), flow velocity in well (green lines), and injection rates from the microhole to the formation (blue lines) along a microhole with a total injection rate of 2 kg/s (dashed lines) and 10 kg/s (solid lines). (For interpretation of the references to colour in this figure legend, the reader is referred to the web version of this article.)

and the radial extent of the cooling zone around a microhole, defined as the radius with a temperature change of 50% and 10% of the total cooling amount after 30 years, is about 1 m and 15 m, respectively. This means that the rock volume from which thermal energy is extracted by conductive preheating is on the order of $10^5$ $m^3$ for the entire microhole array, a volume very small compared to the stimulated reservoir volume, which is on the order of $10^9$ $m^3$. This larger volume of hot rock could potentially be accessed by injecting the working fluid through a microhole array, thus inducing a widely distributed flow pattern in the fracture network.

To quantify the contribution that preheating makes to the overall heat-mining efficiency, we compared the base-case simulation results (see Section 3.2 below) with a case where conductive heat transfer between the formation and the microholes is inhibited. While such a thermal insulation of an open microhole is practically not possible (nor desirable), the analysis provides a bounding case to estimate the maximum impact preheating may have on EGS performance. This analysis shows a thermal energy gain through conductive preheating of about 3.5%. This maximum contribution is small because (1) the total volume accessed by radial conduction toward microholes is relatively small compared to the reservoir volume, as demonstrated above, and (2) conductive preheating extracts additional heat only in borehole sections where no working fluid enters the fracture network. In microhole sections that intersect the reservoir, the working fluid picks up the heat in the vicinity of the microholes and convectively transports it toward the production well, effectively mining the heat from the same volume. Additional heat can only be extracted by preheating occurring within the large-diameter well and those microhole sections that traverse the low-permeability caprock. However, preheating in the large-diameter injection well is minor and partly compensated by corresponding heat losses in the production well. The conclusion that preheating is negligible is obviously particular to the concept described here; preheating may be more effective in other heat-mining concepts, and is the only mechanism relied upon in closed systems commonly used for low-temperature geothermal heat extraction, such as ground source heat pumps.

To further demonstrate the effect of combined conductive and convective processes on preheating, Fig. 4 shows the flow velocity in the microhole (green lines), injection rates from the microhole to the formation (blue lines), and the resulting temperature distribution (red lines) along two microholes, one that takes an average rate of approximately 2 kg/s (dashed lines), and one that takes a high rate of about 10 kg/s (solid lines). Both microholes encounter the fractured reservoir at a depth of about −4400 m, where working fluid starts to be injected into the formation, continuously reducing the velocity in the microhole itself. One of the microholes (solid lines) encounters the wide-aperture zone, which accounts for about 90% of its total injectivity of about 10 kg/s. Unlike the behavior in a cased borehole (as shown in Fig. 3), no sizeable preheating effect can be seen, because the heat is conductively removed from the vicinity of the well (nevertheless contributing to heat mining). Once vertical flow in the microhole ceases near the bottom of the reservoir, the essentially stagnant water heats up to the ambient temperature at that depth (albeit without contributing to heat mining).

Our final consideration is related to self-regulation of a microhole array. The fact that the total amount of injected working fluid is distributed over many microholes provides an opportunity for self-regulation. Unlike in a conventional configuration, where most of the fluid is taken up by one or a few high-injectivity features encountered by the well, microhole arrays are likely to intersect many geological features of varying injectivity. Fractures with high permeability tend to induce high flow velocities in the vicinity of the microhole and in the microhole itself. However, high velocities in the microholes lead to turbulent flow and thus higher flow resistance. As a consequence, as the pressure in one microhole increases, the injected fluid is redistributed to other microholes, resulting in a more even and widespread distribution of injection rates.

To test this hypothesis, we compare the injection-rate distribution using a standard model based on Darcy's law, where potential impacts of inertia and turbulence are neglected, and one based on the Forchheimer (1901) equation, where velocity-dependent flow resistance is accounted for. The non-Darcy flow coefficient is calculated using the model of Geertsma (1974). Accounting for velocity-dependent flow resistance in the microholes, the standard deviation of the flow rates at the head of the 40 microholes is reduced from 2.9 to 1.6 kg/s, indicating a more uniform injection distribution. We conclude that self-regulation of a microhole array reduces the sensitivity of the EGS operation to generally uncertain or unknown heterogeneity in the system, making it more robust.

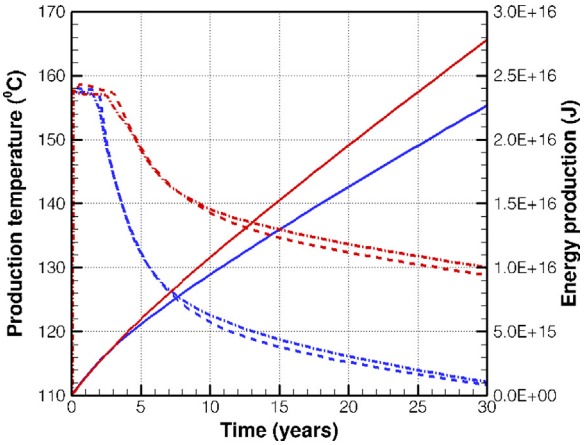


**Fig. 5.** Fluid temperatures at well head of left (dash-dotted lines) and right (dashed lines) production wells for conventional (blue) and microhole (red) configurations. Total produced thermal energy (solid lines). (For interpretation of the references to colour in this figure legend, the reader is referred to the web version of this article.)

### 3.2. Base-case simulation results

We first describe the key simulation results – the temperature of the produced fluid and the total thermal energy extracted from the two wells – for the base-case parameter set and an exploitation period of 30 years. Both configurations – injection through a conventional, central well and injection through an array of microholes – are presented and compared. Fig. 5 shows the temperature evolution of the produced fluid, which is indicative of thermal breakthrough and overall heat mining effectiveness.

The temperature of the produced fluid at very early times is essentially equal to the temperature encountered at the depth of the wide-aperture, high-permeability feature, which is the main feed zone. Temperatures at the well head rise as the relatively colder fluid that is initially in the wells is flushed out, and as the formation in the immediate vicinity of the production wells warms up, reducing heat losses in the upper part of the reservoir and in the 4 km long sections from the reservoir to the surface, as calculated using the semi-analytical approach of Zhang et al. (2011). After this initial temperature increase, colder injection fluid soon reaches the production wells, leading to substantial cooling, specifically for the conventional configuration. The temperatures in the two production wells differ slightly as the feed zones are at different depths due to the inclination of the wide-aperture zone, and due to the fact that their location with respect to the injection well and the geological features are asymmetric. By contrast, injection through a microhole array distributes the fluid over a wider volume of the stimulated reservoir. Flow velocities in the formation are slower, and a larger fraction of the produced water enters the well through the fracture network of the stimulated rock rather than almost exclusively through the wide-aperture feed zones, as is the case for the conventional well configuration. As a result, thermal breakthrough is much less pronounced, and the temperature of the produced fluids at the end of the simulated period is substantially higher (approximately 130 °C) compared to that obtained with the conventional well configuration (approximately 112 °C).

Fig. 5 also shows the cumulative heat extracted from the reservoir, which mirrors the trend of the production temperature as the total flow rate remains essentially constant and (for this system which is essentially closed for fluid flow, but not for heat flow) equal to the injection rate of 80 kg/s. For the base-case scenario, about 23% more energy is produced with the microhole configuration during the 30 year period.

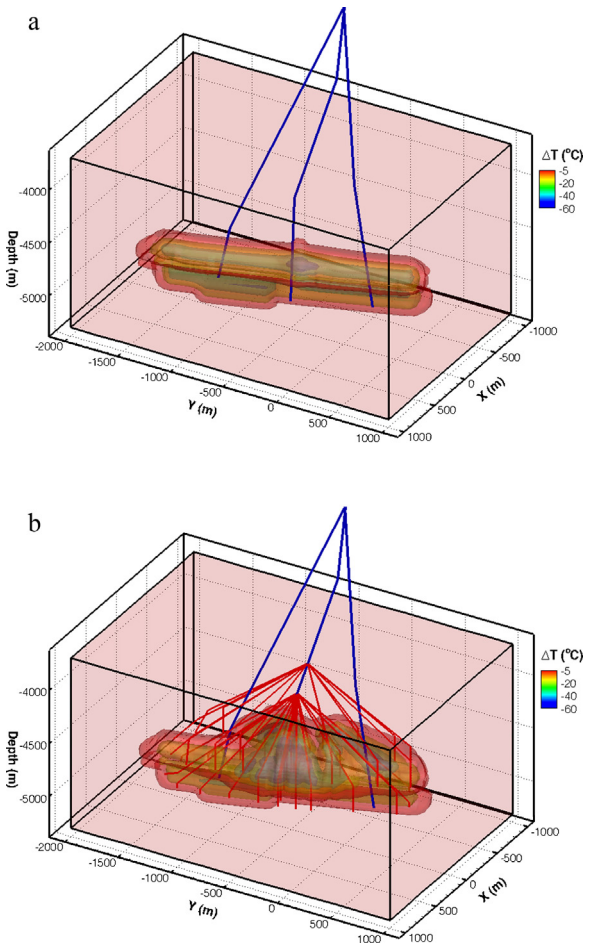


**Fig. 6.** Simulated temperature-change distribution after 30 years of exploitation using (a) conventional and (b) microhole configurations.

Fig. 6 shows the change in reservoir temperature after 30 years of exploitation for both the conventional and microhole configurations. In the conventional well configuration, fluid between the injection and production wells is focused along the wide-aperture zone, limiting heat exchange to a relatively narrow channel. This is clearly visible as an essentially one-dimensional zone of reduced temperature between the injection and production wells. By contrast, injecting the working fluid through a microhole array accesses a larger reservoir volume from which heat can be extracted. The temperature decline in that region, which includes a substantial portion of the fractured reservoir outside the wide-aperture zone, is less severe; this is reflected in the higher temperature of the produced fluid (see Fig. 5).

These base-case simulations seem to support the hypothesis that distributing the working fluid through microholes leads to more effective heat extraction from a larger rock volume, and is less susceptible to the presence of a wide-aperture feature that promotes preferential flow, reduced contact with reservoir matrix, and thus early thermal breakthrough. Note that the configuration of the microhole array (the number of microholes, their length, diameter, orientation, and spatial distribution) has not been optimized for maximum heat mining efficiency. It has been designed based on simple criteria assuming some knowledge about the extent of the stimulated reservoir. A formal optimization of microhole configuration parameters to maximize heat recovery factors will be undertaken in a future analysis.

### 3.3. Local sensitivity analyses

The purpose of the sensitivity analysis is to obtain qualitative insights into the relative importance of the parameters listed in Table 1 for the production of geothermal energy. An influential parameter is one that strongly affects total produced thermal energy. This means that if such a parameter is uncertain, the predicted energy production is also uncertain. While this uncertainty could be beneficial (i.e., lead to higher energy production if the parameter is higher than expected and the related sensitivity coefficient is positive), a system with overall high sensitivity can be considered less robust than one in which uncertainty in hydrogeologic and thermal input parameters does not lead to highly uncertain predictions. We take this view when comparing the robustness of the conventional and microhole well designs. Specifically, as discussed in the previous subsection, EGS based on microhole arrays has overall a better heat mining efficiency than a conventional well configuration for the base-case parameter set. The sensitivity analysis will shed some light on whether this result is robust to changes in uncertain parameters.

In this section, we will briefly discuss results from a standard local sensitivity analysis, focusing on a few influential parameters. The local sensitivity analysis assesses the effect of a perturbation of an individual parameter from its base-case value. In the next section, the results of a global sensitivity analysis are presented in more detail.

The relative magnitude of the local sensitivity coefficient indicates that the injection rate is the most influential parameter for both the conventional and microhole system. This is expected as the injection rate directly affects the circulation and production rates and consequently determines the amount of thermal energy extracted from the reservoir. Fortunately, this parameter can be controlled, and is thus not crucial for affecting prediction uncertainty, but gives a reference value for the sensitivity analysis. In the conventional design, horizontal fracture permeability is the most influential parameter, as it determines how much water gets in contact with hot rock matrix outside of the wide-aperture zone, whose permeability is also influential. Unless the extent and properties of this zone are well characterized, EGS performance may be difficult to predict reliably. In contrast, the microhole injection design essentially forces circulation through the fracture network, so its permeability is of less importance, whereas the fracture-matrix area reduction factor plays a more significant role in picking up thermal energy from the rock matrix. This analysis implies that if a fast flow path exists, its properties and that of the surrounding fracture network are essential parameters to know if the EGS is operated conventionally, whereas a microhole-based design is less affected by uncertainties in fracture permeability and the existence of a wide-aperture zone.

Finally, the microhole case shows comparable sensitivities to horizontal and vertical fracture permeability, whereas the conventional case shows high sensitivity to the horizontal permeability, but almost no sensitivity to vertical permeability, reflecting the fact that injection through microholes results in a more three-dimensional flow field.

The sensitivity coefficients of some parameters change sign between early- and late-time behavior. For example, larger fracture spacing and smaller interface area reduction factor initially lead to higher energy production as more of the injected fluid travels to the production wells rather than flowing into the matrix. This initial advantage, however, is quickly reversed at later times, when the reduced fracture-matrix surface area limits heat mining efficiency. Other parameters (such as thermal conductivity and specific heat) always show a positive sensitivity coefficient during the entire exploitation period, indicating that an increase in these parameter values always leads to higher energy production.

The analysis of the covariance matrices reveals strong correlations among all permeability estimates, as expected. In particular, relatively strong correlations are observed between fracture permeability and wide-aperture zone permeability for the conventional well configuration, i.e., a change in permeability for one of these features can be partly compensated for by a change in the other, leading to similar energy productions. If using microholes, however, this correlation is much weaker, indicating that the flow paths through the wide-aperture zone and those through the stimulated fracture network are fundamentally different and do not allow for a linear compensation. This can be interpreted as the microhole array being less influenced by the presence or properties of a preferential flow path, which makes the microhole design more robust. There are also fairly strong correlations between fracture spacing and fracture-matrix area reduction factor as well as the thermal properties. Such correlations also affect the uncertainty of the predicted thermal energy production.

In summary, the sum of all absolute values of the sensitivity coefficients for microhole-based EGS is less than that of a conventional design despite the higher energy production. This can be interpreted as microholes reducing uncertainty in predicted system behavior and thus providing a more robust design. Moreover, parameter correlations are weaker for the proposed microhole design compared to those of a conventional well configuration. This may be essential when characterizing the EGS reservoir using data from production or observation wells, with weaker correlations generally leading to more accurate estimates.

### 3.4. Global sensitivity analyses

The sensitivity analysis discussed in the previous subsection is local in that it refers to the base-case parameter set only. For highly nonlinear models – such as the models described here – sensitivity coefficients may change drastically if evaluated at different points in the high-dimensional parameter space. For example, we made assumptions about the properties of a wide-aperture zone. Simply its existence affects the results of the sensitivity analysis of all parameters considered uncertain. Moreover, once the permeability of this zone becomes sufficiently large, a further increase of its value may no longer affect the predicted energy production; furthermore, if its permeability is relatively small and similar to that of the background fracture network, its influence may also be negligible. Only if the wide-aperture-zone permeability is in an intermediate range may it have the impact we have seen for the conventional case. This behavior has been confirmed by evaluating the energy production over a wide range of permeabilities for the wide-aperture zone. Moreover, the existence and properties of the wide-aperture zone impacts the sensitivity coefficients of all the other parameters as a result of correlations.

As outlined in Section 2.3, so-called global sensitivity analysis methods examine sensitivity coefficients over a wide section of the parameter space and evaluate an average elementary effect of each parameter. The standard deviation of the elementary effect is a measure of inherent nonlinearities and potential dependencies among the parameters. Here, the elementary effect is calculated based on total heat production over a ten-year production period; only its relative value should be interpreted.

Fig. 7 shows the mean of the absolute elementary effect against its standard deviation calculated using the method of Morris (1991). A total of 168 parameter combinations are evaluated within the ranges shown in Table 1, using the Morris scheme with six partitions and 12 paths. Parameters to the right of the plot have an overall high influence on the predicted EGS performance; parameters with a high standard deviation relative to the mean elementary effect (i.e., those plotting above the dashed unit-slope line) show

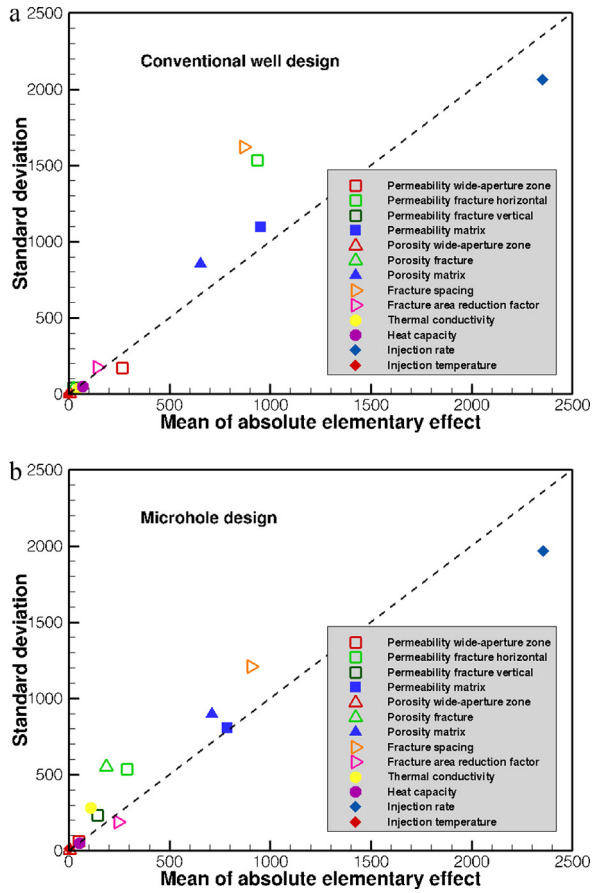


**Fig. 7.** Elementary effect and standard deviation of parameters examined using Morris global sensitivity analysis results for (a) conventional injection well, and (b) microhole arrays. Parameters plotting above the dashed line exhibit relatively strong nonlinearity effects or include dependencies to other parameters.

relatively strong nonlinearity effects or include dependencies to other parameters.

For the case with a conventional injection well (Fig. 7a), the Morris analysis indicates that the horizontal fracture permeability is the most influential parameter (we do not further comment on the injection rate, as it is a controllable parameter). Unlike the result from the local sensitivity analysis, the permeability of the wide-aperture zone is of intermediate importance, because (as discussed above) the sensitivities at very low or very high values are small, resulting in a reduced mean elementary effect. Fracture spacing and horizontal fracture permeability are moderately influential parameters with relatively strong dependencies and nonlinear effects. Matrix properties on average also affect the predicted heat production notably. This relatively high influence is likely a result of the large range over which matrix permeability is evaluated, where the high values include the impact of smaller fractures that are not accounted for in the fracture continuum. Heat capacity of the reservoir rock is of relatively low importance, and shows only weak dependencies over the narrow range it is allowed to vary.

For the case with a microhole array used for injection of the EGS working fluid, the global sensitivity analysis also reveals that nonlinearities and correlations are present, as indicated by most symbols plotting above the unit-slope line on Fig. 7b. Nevertheless, fracture spacing remains a key parameter, as it directly affects the total fracture-matrix interface area), followed by matrix properties and the permeability of the fracture network in both horizontal and vertical directions. The fracture-matrix area reduction factor is of similar influence, but shows a more linear or independent behavior, which may be a result of the fact that it only affects the local exchange of fluid and heat between the fractures and the matrix rather than the global flow pattern.

The global sensitivity analysis, while of qualitative nature, provides additional insights into the relative importance of parameters and their dependencies, evaluated over the feasible parameter space rather than only at the base-case point. Since the predicted heat production depends nonlinearly on various combinations of the 13 parameters considered in this study, their relative influence is very difficult to assess based on physical insights into the impact of individual parameters or pairs of directly correlated parameters alone. Global sensitivity analysis using the Morris method, which is applicable even for computationally very demanding models, appears to be a valuable tool to evaluate EGS performance under uncertainty.

## 4. Conclusions

The success and sustainability of energy production from enhanced geothermal systems largely depends on the ability of the working fluid to get in contact with a substantial volume of hot reservoir rock. Large-scale stimulation of existing fractures or creation of a new fracture system with sufficient density and connectivity is a prerequisite. However, even if such stimulation is successful, the pressure field induced by a conventional well configuration, where cold water is injected at discrete locations of a small number of injection wells, and produced from a few feed zones in production wells, the fracture surface and thus the volume of the heat-storing reservoir accessed by the working fluid may be very limited.

The flexibility offered by microhole drilling technology enables installation of a large number of boreholes from a central well in a configuration that allows for distributed injection (or production) of geothermal working fluids. Such a configuration has the potential to (1) increase the probability of intersecting flowing fractures, (2) increase the fracture surface area contacted by circulating water and thus increase the volume of rock accessible for heat mining, (3) reduce the risk of flow channeling and early thermal breakthrough, (4) increase the preheating of the working fluid as it flows from the surface to the injection point, and (5) provide for self-regulated distributions of injection rates.

The generic modeling study presented here indicates that EGS based on microhole arrays could significantly increase heat mining rates and their sustainability over longer time periods. Moreover, the sensitivity analysis shows that the proposed well configuration is more robust to uncertainties in key hydrological and thermal parameters, thus reducing the risk of encountering unexpected performance.

While the study has examined the general concept and showed the potential benefits of microhole-based EGS, its viability strongly depends on the technical feasibility and costs of drilling microhole arrays from a central, conventionally drilled large-diameter well. Great advances have been made in horizontal and directional drilling, opening up opportunities for additional well configurations that support the overall goal of increasing the accessible rock volume. Stimulation of that rock volume is another key issue that may benefit from the flexibility offered by advanced drilling technologies and multiple wells emplaced with an optimized configuration. Some of these issues will be addressed in future research.

## Acknowledgments

The very thoughtful comments and suggestions by two anonymous reviewers and the technical review by Yoojin Jung of Lawrence Berkeley National Laboratory are greatly appreciated.

This work was supported by Lawrence Berkeley National Laboratory under U.S. Department of Energy, Assistant Secretary for Energy Efficiency and Renewable Energy, Geothermal Technologies Program, Contract No. DE-FOA-0000075: Recovery Act: Enhanced Geothermal Systems Component Research and Development/Analysis, and DE-AC02-05CH11231.

## Appendix A. Governing equations

TOUGH2 (Pruess et al., 1999) is a numerical simulator of nonisothermal, multiphase, multicomponent flows in fractured porous media. In what follows, we limit the description to nonisothermal flow of a single component (water) in a single (the liquid) phase, which is the fluid system considered in this simulation study. The basic mass- and energy balance equations solved by TOUGH2 for this system can be written in the general form

$$\frac{d}{dt}\int_{V_n} M^K dV_n = \int_{\Gamma_n} \mathbf{F}^K \mathbf{n} d\Gamma_n + \int_{V_n} q^K dV_n \quad (A.1)$$

The integration is over an arbitrary subdomain $V_n$ of the flow system under study, which is bounded by the closed surface $\Gamma_n$. The quantity M appearing in the accumulation term (left hand side) represents the mass of water (K = w) or energy (K = h) per volume. **F** denotes mass or heat flux, and q denotes sinks and sources; **n** is a normal vector on surface element $d\Gamma_n$, pointing inward into $V_n$.

The general form of the mass accumulation term is

$$M = \phi\rho \quad (A.2)$$

where $\phi$ is porosity, and $\rho$ is the density of water as a function of pressure and temperature.

Advective mass flux is given by Darcy's law:

$$\mathbf{F} = \rho\mathbf{u} = -k\frac{\rho}{\mu}(\nabla P - \rho\mathbf{g}) \quad (A.3)$$

Here **u** is the Darcy velocity (volume flux), k is absolute permeability, $\mu$ is viscosity, P is pressure, **g** is the vector of gravitational acceleration.

Heat flux includes conductive and convective components

$$\mathbf{F}^h = -\lambda\nabla T + h\mathbf{F} \quad (A.4)$$

where $\lambda$ is thermal conductivity, and h is specific enthalpy in the liquid phase.

All water properties (density, specific enthalpy, viscosity, saturated vapor pressure) are calculated from the steam table equations as given by the International Formulation Committee (1967). Density and internal energy are represented within experimental accuracy. Viscosity of liquid water and steam are represented to within 2.5% by correlations given in the same reference.

For numerical simulation the continuous space and time variables must be discretized. Space discretization is made directly from the integral form of the basic conservation equations (Eq. (A.1)), without converting them into partial differential equations. This "integral finite difference" method (IFDM; Narasimhan and Witherspoon, 1976) avoids any reference to a global system of coordinates, and thus offers the advantage of being applicable to regular or irregular discretizations in one, two, and three dimensions. Time is discretized fully implicitly as a first-order backward finite difference.

The discretization results in a set of strongly coupled nonlinear algebraic equations, with the time-dependent primary thermodynamic variables of all grid blocks as unknowns. These equations are cast in residual form and are solved simultaneously using Newton–Raphson iteration. Different methods are available to solve the linear equations arising at each iteration step, including preconditioned conjugate gradient solvers, as well as sparse direct matrix methods.

To model fractured porous media (as a stimulated geothermal reservoir), a dual-permeability approach is used. Matrix blocks of low permeability are embedded in a network of interconnected fractures. Global flow in the reservoir occurs mainly through the fracture system, which is described as an effective porous continuum. Rock matrix and fractures may exchange fluid (or heat) locally, driven by the difference in pressures (or temperatures) between matrix and fractures, which in this study is assumed as being quasi-steady, with rate of matrix-fracture interflow proportional to the difference in (local) average pressures (or temperatures). Generation of the fracture and matrix continua and their interconnection is a geometrical pre-processing step that operates on the element and connection data of a porous medium mesh to calculate—for given data on volume fractions—the volumes, interface areas, and nodal distances for a secondary fractured medium mesh. The information on fracturing (spacing, number of sets, shape of matrix blocks) required for this is provided by a proximity function, which expresses, for a given reservoir domain $V_o$, the total fraction of matrix material within a distance from the fractures. Details about the dual-continuum approach, its applicability and limitations can be found in Pruess and Narasimhan (1982; 1985), Pruess et al. (1999) and Doughty (1999).

## References

Albright, J.N., Dreesen, D.S., 2000. Microhole technology lowers reservoir exploration, characterization costs. Oil and Gas Journal 98 (2), 39–41.

Cuenot, N., Dorbath, C., Dorbath, L., 2008. Analysis of the microseismicity induced by fluid injections at the EGS Site of Soultz-sous-Forêts (Alsace, France): Implications for the characterization of the geothermal reservoir properties. Pure and Applied Geophysics 165, 797–828.

Doughty, C., 1999. Investigation of conceptual and numerical approaches for evaluating moisture, gas, chemical, and heat transport in fractured unsaturated rock. Journal of Contaminant Hydrology 38 (1–3), 69–106.

Finger, J., Jacobson, R., Hickox, C., Combs, J., Polk, G., Goranson, C., 1999. Slimhole Handbook: Procedures and Recommendations for Slimhole Drilling and Testing in Geothermal Exploration. Report SAND99-1076, Sandia National Laboratories, Albuquerque, New Mexico, USA, 164 pp.

Finsterle, S., 1998. Parallelization of iTOUGH2 Using PVM. Report LBNL-42261, Lawrence Berkeley National Laboratory, Berkeley, California, USA, 37 pp.

Finsterle, S., 2004. Multiphase inversion modeling: review and iTOUGH2 applications. Vadose Zone Journal 3, 747–762.

Finsterle, S., Zhang, Y., 2011. Solving iTOUGH2 simulation and optimization problems using the PEST protocol. Environmental Modelling and Software 26, 959–968, http://dx.doi.org/10.1016/j.envsoft.2011.02.008.

Forchheimer, P., 1901. Wasserbewegung durch Boden. Zeitschrift Verein Deutscher Ingenieure 45, 1782–1788.

Garg, S.K., Combs, J., 1997. Use of slim holes with liquid feedzones for geothermal reservoir assessment. Geothermics 26 (2), 153–178.

Garg, S.K., Combs, J., 2002. A Study of Production/Injection Data from Slim Holes and Large-Diameter Wells at the Okuaizu Geothermal Field, Tohoku, Japan. Report INEEL/EXT-02-01429, Idaho National Engineering and Environmental Laboratory, Idaho, USA, 257 pp.

Garg, S.K., Combs, J., 2010. Appropriate use of USGS volumetric heat in place method and Monte Carlo calculations. In: Proceedings of the 34th Workshop on Geothermal Reservoir Engineering, Stanford University, Stanford, California, USA, pp. 80–86.

Gérard, A., Kappelmeyer, O., 1987. The Soultz-sous-Forêts project. Geothermics 16 (4), 393–399.

Geertsma, J., 1974. Estimating the coefficient of inertial resistance in fluid flow through porous media. Society of Petroleum Engineers Journal, 445–450.

Grant, M.A., Garg, S.K., 2012. Recovery factor for EGS. In: Proceedings of the 37th Workshop on Geothermal Reservoir Engineering, Stanford University, Stanford, California, USA, pp. 738–740.

Heuze, F., 1995. Slimhole Drilling and Directional Drilling for On-Site Inspections Under a Comprehensive Test Ban – An Initial Assessment. Report UCRL-ID-121295. Lawrence Livermore National Laboratory, Livermore, California, USA, 16 pp.

International Formulation Committee, 1967. A Formulation of the Thermodynamic Properties of Ordinary Water Substance. IFC Secretariat, Düsseldorf, Germany, 34 pp.

Johnson, M.O., Hyatt, P.G., 2005. Unique through tubing completions maximize production and flexibility. SPE Paper 92392, Presented at the SPE/IDC Drilling Conference, Amsterdam, The Netherlands, 23–25 February, http://dx.doi.org/10.2118/92392-MS

Liu, H.H., Doughty, C., Bodvarsson, G.S., 1998. An active fracture model for unsaturated flow and transport in fractured rocks. Water Resources Research 34 (10), 2633–2646.

Maurer, W.C., 1980. Advanced Drilling Techniques. Petroleum Publishing Company, Tulsa, OK, USA, ISBN 0-87814-117-0, 698 pp.

McDermott, C.I., Randriamanjatosoa, A.R.L., Tenzer, H., Kolditz, O., 2006. Simulation of heat extraction from crystalline rocks: the influence of coupled processes on differential reservoir cooling. Geothermics 35 (3), 321–344.

Michelet, S., Toksöz, M.N., 2007. Fracture mapping in the Soultz-sous-Forêts geothermal field using microearthquake locations. Journal of Geophysical Research 112, B07315, 14, http://dx.doi.org/10.1029/2006JB004442.

MIT, 2006. The Future of Geothermal Energy – Impact of Enhanced Geothermal Systems (EGS) on the United States in the 21st Century. MIT Press, Boston, USA, 372 pp.

Moe, H., Rabben, K., 2001. Plant for Exploiting Geothermal Energy, US Patent 6,247,313.

Morris, M.D., 1991. Factorial sampling plans for preliminary computational experiments. Technometrics 33 (2), 161–174.

Narasimhan, T.N., Witherspoon, P.A., 1976. An integrated finite difference method for analyzing fluid flow in porous media. Water Resources Research 12, 57–64.

Oglesby, K., 2009. Advanced Mud System for Microhole Coiled Tubing Drilling, Final Technical Report, DE-FC26-04NT15476, 97 pp.

Pan, L., Oldenburg, C.M., Pruess, K., Wu, Y.S., 2011. Transient $CO_2$ leakage and injection in wellbore-reservoir systems for geologic carbon sequestration. Greenhouse Gases: Science and Technology 1 (4), 335–350.

Pritchett, J.W., 1998. Electrical Generating Capacities of Geothermal Slim Holes. Report MTSD-DFR-98-16223, Maxwell Technologies Systems Division, Inc., San Diego, California, USA, 7 pp.

Pruess, K., Narasimhan, N.T., 1982. On fluid reserves and the production of superheated steam from fractured, vapor-dominated geothermal reservoirs. Journal of Geophysical Research 87 (B11), 9329–9339.

Pruess, K., Narasimhan, N.T., 1985. A practical method for modeling fluid and heat flow in fractured porous media. Society of Petroleum Engineers Journal 25 (1), 1567–1578.

Pruess, K., Oldenburg, C., Moridis, G., 1999. TOUGH2 User's Guide, Version 2.0. Report LBNL-43134, Lawrence Berkeley National Laboratory, Berkeley, California, USA, 210 pp.

Saltelli, A., Ratto, M., Andres, T., Campolongo, F., Cariboni, J., Gatelli, D., Saisana, M., Tarantola, S., 2008. Global Sensitivity Analysis, The Primer. John Wiley & Sons Ltd., West Sussex, England, 292 pp.

Sanyal, S.K., Butler, S.J., 2005. An analysis of power generation prospects from enhanced geothermal systems. Transactions Geothermal Resources Council 29, 131–138.

Sanyal, S.K., Granados, E.E., Butler, S.J., Horne, R.N., 2005. An alternative and modular approach to enhanced geothermal systems. Transactions Geothermal Resources Council 29, 139–144.

Sausse, J., Dezayes, C., Dorbath, L., Genter, A., Place, J., 2010. 3D model of fracture zones at Soultz-sous-Forêts based on geological data, image logs, induced microseismicity and vertical seismic profiles. Comptes Rendus Geoscience 342, 531–545.

Stauffer, P.H., Stein, J.S., Travis, B.J., 2003. The Correct Form of the Energy Balance for Fully Coupled Thermodynamics in Liquid Water, Report LA-UR-03-1555, Los Alamos National Laboratory, Los Alamos, New Mexico, USA, 9 pp.

Summers, D., Oglesby, K., Galecki, G., Woelk, K., 2007. Method and Apparatus for Jet-Assisted Drilling and Cutting, US patent application 12/400,507; pending.

Vogt, C., Kosack, C., Marquart, G., 2012. Stochastic inversion of the tracer experiment of the enhanced geothermal system demonstration reservoir in Soultz-sous-Forêts – Revealing pathways and estimating permeability distribution. Geothermics 42, 1–12.

Warren, J.E., Root, P.J., 1963. The behavior of naturally fractured reservoirs. Society of Petroleum Engineering Journal 228, 245–255.

Zhang, Y., Pan, L., Pruess, K., Finsterle, S., 2011. A time-convolution approach for modeling heat exchange between a wellbore and surrounding formation. Geothermics 40 (4), 251–266, http://dx.doi.org/10.1016/j.geothermics.2011.08.003.